Orientational glass transition in a rotator model

C. Renner,[1] H. Löwen,[1] and J. L. Barrat[2]
[1]*Sektion Physik der Universität München, Theresienstrasse 37, D-80333 München, Germany*
[2]*Département de Physique des Matériaux (URA CNRS 172), Université Claude Bernard-Lyon I, 43, Boulevard du 11 Novembre, F-69622 Villeurbanne Cedex, France*
(Received 11 April 1995)

Orientational dynamics in a simple model of infinitely thin hard needles, initially proposed by Rubinstein and Obukhov [1], are investigated by molecular dynamics simulations. The center-of-mass coordinates of the needles are fixed on a regular fcc lattice. The statics of the system is analytically known, yielding a global stability of the disordered phase. The dynamical properties, however, are nontrivial. As the ratio l of needle length to lattice constant is increased, the time scale for the decay of orientational correlations increases rapidly. A "computer glass transition" is observed in the vicinity of $l \approx 2.7$, with the orientational correlations being frozen-in on the time scale of our simulation. The scenario for this glass transition is very similar to that observed in conventional structural or orientational glasses. The glass transition in the rotator model, however, is *necessarily a purely dynamical feature,* since the static properties of the system are known to be independent of l. The same glass transition is also studied in a system confined between two parallel plates, for various boundary conditions at the plates. The transition is found to take place for the same value of l as in the bulk, provided the number of possible collision partners near the boundary is the same as in the bulk.

PACS number(s): 64.70.Pf, 61.20.Ja

I. INTRODUCTION

In the past 15 years, structural and orientational relaxations in glass-forming materials have been thoroughly analyzed experimentally, theoretically in the framework of mode-coupling theories [2], and by computer simulation of simple models [3]. Evidence has been presented that the dynamical relaxation in structural [4] and orientational [5–7] glasses is a multistep mechanism, in which at least two different time scales are involved. As the system becomes more strongly coupled (either by cooling or by compression), these time scales appear to diverge critically near a state point associated with a "kinetic glass transition." The relaxation near this state point exhibits some universal features, which are described in Refs. [8,9].

A direct insight into the principles of glass formation is gained by studying simple models for one-component glass formers, allowing a direct comparison with theoretical predictions. Notable success has been achieved for the simple hard-sphere fluid, which can be compressed to exhibit an amorphous glassy phase, as seen experimentally in samples of sterically stabilized colloidal suspensions. Although there seems to be quite good agreement between the experimental data and the predictions of mode-coupling theory [10], details of the density relaxation are still controversial. The hard-sphere system has the advantage that its fluid equilibrium structure and its phase diagram are independent of temperature and depend only on the volume fraction of the spheres. From computer simulation it is known that the hard-sphere fluid crystallizes into a regular crystal if the volume fraction is larger than 0.494 [11]. The glass transition, however, takes place at a significantly higher packing fraction of about 0.62. Hence it is a nonequilibrium effect, associated with a *metastable* fluid phase.

The aim of the present paper is to study another very simple model, which was proposed by Rubinstein and Obukhov [1] as a good candidate for an "ideal" glass transition. The system is made of rotators whose equilibrium structure and phase behavior are known *exactly* but whose dynamical features are nontrivial. Basically it is a hard-needle model, with elastic collisions between the needles and free rotator dynamics between the collisions. The center-of-mass coordinates of infinitely thin needles with a classical orientational degree of freedom are fixed onto space points of a regular fcc crystal. The only parameter characterizing the system is the ratio l of the needle length L to the lattice constant a. The static properties of the system are trivial and identical to those of free rotators since the volume of the needles is strictly zero. Hence also the bulk phase diagram is trivial, yielding a *global* stability of the orientationally disordered phase. The *dynamics* of the rotators, however, is nontrivial since the needles cannot cross each other. To our knowledge there are no analytical results for dynamical correlations in this system. In this paper, numerical simulations will be used to obtain the time-dependent orientational correlation functions of the model.

The model can also be considered as a caricature for orientational glasses. The usual modeling of these glasses involves molecules rotating around fixed lattice positions and carrying dipoles or quadrupoles. Hence, as the relatively simple hard-sphere model is the "prototype" for a structural glass transition, the even simpler rotator model may be regarded as a suitable prototype for orientational glasses.

The interest in the dynamical features of the rotator model stems from the possibility of observing a glass transition that would unambiguously have a purely

dynamical origin, without any underlying singularity in the static properties. There is a strong suspicion that, in simple liquids, the glass transition also has a purely dynamical origin. The static properties in liquids, however, are known only from approximate theories, so that the existence of singularities that would be missed by these theories cannot be excluded. Besides this obvious fundamental advantage, the simplicity of the static properties in the rotator model also involves a huge practical advantage in computer simulations. In simple liquids, the necessity for very long equilibration times after each cooling step in order to reach a typical equilibrium configuration constitutes the main bottleneck for computer simulations near the glass transition [12,13]. For the rotator model, an equilibrium configuration is generated instantaneously by assigning random orientations and Maxwellian-distributed angular velocities to each rotator. As a consequence, the cooling rate dependence that systematically affects simulation results for conventional glass formers is absent in the rotator model.

The paper is organized as follows. Section II presents a detailed description of the rotator model. The details of the simulations are summarized in Sec. III. The results of the simulation for bulk systems are described in Sec. IV. Our main result here is the occurrence of an orientational glass transition for a finite value of l. In Sec. V, we take advantage of the simplicity of the rotator model to extend our study of the glass transition to the case of a confined geometry, a subject of current experimental [14–16] and theoretical [17] interest. The orientational correlations are studied and compared to those in the bulk for a system confined between two parallel plates, with various boundary conditions. A summary and discussion of the results are given in Sec. VI.

II. ROTATOR MODEL

We consider N infinitely thin, hard needles of length L with a homogeneous line mass density m/L whose center-of-mass coordinates $\{\vec{r}_i\}$ $(i=1,\ldots,N)$ are fixed onto sites of a regular three-dimensional lattice. For our calculations we have chosen an fcc lattice, but it is strongly expected that a different lattice structure will not destroy the qualitative features of the model. One configuration of the rotators is specified by their orientations, conveniently given by a set of unit vectors $\{\vec{u}_i\}$ $(i=1,\ldots,N)$, and their angular velocities $\{\vec{\omega}_i\}$ $(i=1,\ldots,N)$. Since the needles are infinitely thin, the angular velocities are perpendicular to the orientations:

$$\vec{u}_i\cdot\vec{\omega}_i=0, \quad i=1,\ldots,N \ . \tag{1}$$

The angular momenta $\{\vec{L}_i\}$ $(i=1,\ldots,N)$ are related to the angular velocities by $\vec{L}_i=\tilde{\Theta}\vec{\omega}_i$, where $\tilde{\Theta}$ is the tensor of inertia whose values on the principal needle axis are $(0,J,J)$ with $J=mL^2/12$. The geometry is visualized in Fig. 1. If the needle length is smaller than the nearest-neighbor distance $a/\sqrt{2}$ in the lattice, the needles are an ensemble of noninteracting free rotators. However, for $l=L/a>1/\sqrt{2}$, collisions between the rotators are possible, which we describe further in Sec. II B.

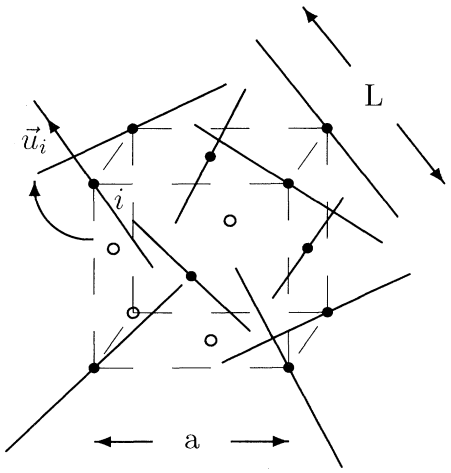

FIG. 1. Unit cell (dashed line) of the underlying fcc lattice together with the needles of length L whose center-of-mass positions are fixed to lattice sites. The lattice sites are the black and the open circles. In the latter case no needles are drawn for the sake of clarity. Also shown are the lattice constant a and the orientational unit vector $\vec{u}_i$ of a rotating needle, labeled by the index i.

A. Statics of the rotator model

The excluded volume occupied by the needles is zero. Consequently the classical partition function can be calculated analytically [18]. As a result, in the canonical ensemble the free energy per particle $f\equiv F/N$ is

$$f=-k_BT\ln\left[\frac{8\pi^2Jk_BT}{h^2}\right], \tag{2}$$

where T is the temperature and k_B denotes Boltzmann's and h Planck's constant. The thermal energy k_BT serves to define the natural "microscopic" time scale τ in the model. Henceforth all times are measured in this unit, where

$$\tau=\sqrt{J/2k_BT}\equiv\sqrt{mL^2/24k_BT} \ . \tag{3}$$

One easily observes that, in the thermodynamic limit $N\to\infty$, f is an analytical quantity. This implies that there is no structural bulk phase transition in the model. The system always prefers the orientationally disordered phase; a nematiclike or liquid-crystalline phase is not stable over the whole range of needle lengths. Furthermore, any structural correlations factorize, since the rotators are essentially decoupled for the statics. For instance, the orientations of two neighboring rotators are fully independent.

B. Dynamics

The dynamics of the system are specified by the collision rules between the rotators [18]. The dynamics result in time-dependent orientations and angular velocities, i.e., in a set of trajectories $\{\vec{u}_i(t)\},\{\vec{\omega}_i(t)\}$. The collisions are assumed to happen instantaneously; i.e., the

angular velocities are piecewise constant as a function of time. A collision between two needles i and j takes place at time t if there are two real numbers α and β with a modulus less than $L/2$, such that

$$\vec{r}_i-\vec{r}_j+\alpha\vec{u}_i(t)-\beta\vec{u}_j(t)=\vec{0}\ . \tag{4}$$

Here α measures the distance of the collision point from the center-of-mass coordinate of rod i, and β is the distance to the center-of-mass coordinate of particle j. Equation (4) can be easily solved, resulting in

$$\alpha=-\frac{\vec{r}_{ij}\cdot\vec{u}_i-(\vec{r}_{ij}\cdot\vec{u}_j)(\vec{u}_i\cdot\vec{u}_j)}{1-(\vec{u}_i\cdot\vec{u}_j)^2} \tag{5}$$

and

$$\beta=\frac{\vec{r}_{ij}\cdot\vec{u}_j-(\vec{r}_{ij}\cdot\vec{u}_i)(\vec{u}_i\cdot\vec{u}_j)}{1-(\vec{u}_i\cdot\vec{u}_j)^2}\ , \tag{6}$$

where $\vec{r}_{ij}\equiv\vec{r}_i-\vec{r}_j$. The needles do not exert any friction forces during the collision, which directly implies that the momentum exchanged during a collision is perpendicular to the rod orientations. Hence we can write the momentum transfer $\Delta\vec{p}$ after a collision as

$$\Delta\vec{p}=\Delta p\frac{\vec{u}_i\times\vec{u}_j}{|\vec{u}_i\times\vec{u}_j|}\ . \tag{7}$$

The corresponding change in the angular momenta of the colliding needles i and j is given by

$$\Delta\vec{L}_i=\alpha\vec{u}_i\times\Delta\vec{p} \tag{8}$$

$$\Delta\vec{L}_j=-\beta\vec{u}_j\times\Delta\vec{p}\ . \tag{9}$$

The collision rules are completed by specifying Δp using conservation of total energy. This yields [19]

$$\Delta p=\frac{2}{\alpha^2+\beta^2}\frac{(\vec{u}_i\times\vec{u}_j)}{|\vec{u}_i\times\vec{u}_j|}\cdot(\beta\vec{L}_j\times\vec{u}_j-\alpha\vec{L}_i\times\vec{u}_i)\ . \tag{10}$$

Here $\vec{L}_i$ and $\vec{L}_j$ are the angular momenta *before* the collision.

The collision dynamics is nontrivial. In contrast to the collision dynamics of hard spheres, where the collision times can be calculated analytically [20], one has to solve the transcendental equation (4) for the collision time t numerically. An efficient algorithm developed by Frenkel and Maguire [18] was used in our study. Frenkel and Maguire, however, considered a different system of hard needles, where the center-of-mass motion is not frozen-in as it is in our lattice model. Furthermore, Frenkel and Maguire did not address the glass transition in this model.

III. COMPUTER SIMULATION OF THE ROTATOR MODEL

The system that was simulated is a cubic cell containing $N=500$ needles, with periodic boundary conditions. In the initial configuration, the needles are given random orientations $\{\vec{u}_i\}\equiv\{\vec{u}_i(0)\}$ $(i=1,\ldots,N)$ and angular velocities $\{\vec{\omega}_i\}\equiv\{\vec{\omega}_i(0)\}$ $(i=1,\ldots,N)$, such that Eq. (1) is guaranteed and the mean square $\langle\vec{\omega}^2\rangle$ is given by $1/\tau^2=24k_BT/mL^2$. The collision times are computed by solving Eq. (4) for all particle pairs, such that their distance is less than L. At each collision, the angular velocities of the colliding needles are modified according to the rules defined in Sec. II B, and the collision times are updated. The actual implementation was strongly inspired by the algorithm of Frenkel and Maguire [18]; details are given in Ref. [19]. As mentioned above, the arbitrarily chosen initial configuration is an equilibrium configuration in the needle model, so that an equilibration period is not required as long as the angular velocities are taken from a Maxwell distribution. The time-dependent correlation function can be computed accurately by letting the system evolve from its initial configuration for a sufficiently long time T. Typically T was several hundred microscopic times τ.

The ratio $l=L/a$ was varied between 1 and 4.5. The number of possible collision partners N_N grows rapidly with increasing l, approximately following a power-law $N_N\propto l^3$. The computational effort thus grows rapidly with increasing l, since the number of collisions during a given time interval increases. In Fig. 2 the mean collision time t_c, i.e., the average time between two consecutive collisions in our finite-size system, is shown as a function of l. This time decreases rapidly for increasing l (note the logarithmic scale for t_c/τ).

The sensitivity of our results to finite-size effects was checked by running the same simulation for systems made of $N=256$, 864, and 2048 needles. Comparing the results for several dynamical correlation functions, it was found that $N=500$ particles are sufficient for $L/a\leq 4$. Hence finite-size effects are only relevant for large l $(l>4)$, far away from any dynamical glass transition. The numerical accuracy of the simulation was also checked by performing the following test. The final configuration of a trajectory generated over a long time interval (10^4–10^5 collisions) was taken as a starting configuration, with reversed angular velocities. In this "reversed" trajectory, the inverted sequence of collisions should be identical to that of the original trajectory. This was indeed the case even over a long time interval and for a large value of l, provided double-precision numbers are used.

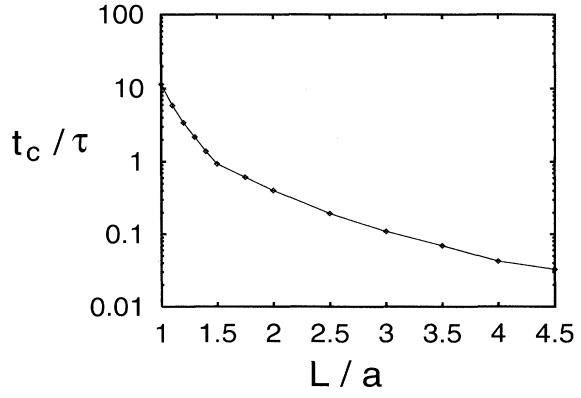

FIG. 2. Mean collision time t_c in units of the microscopic time scale τ on a logarithmic scale versus ratio $l=L/a$.

IV. RESULTS FOR THE BULK ORIENTATIONAL GLASS TRANSITION

A. Dynamical correlation functions

Nontrivial dynamical correlations are contained in the time-autocorrelation functions for the needle orientations and their angular velocities. The orientation-autocorrelation function $\phi_1(t)$ is defined via

$$\phi_1(t)=\left\langle \frac{1}{N}\sum_{i=1}^{N}\vec{u}_i(0)\cdot\vec{u}_i(t)\right\rangle , \tag{11}$$

where $\langle\ \rangle$ denotes a canonical average. For a free rotator in the canonical ensemble, this autocorrelation function can be calculated analytically, yielding

$$\phi_1(t)\equiv\phi_1^f(t)=1-\frac{t}{\tau}\exp\left[-\frac{t^2}{4\tau^2}\right]\tilde{\Phi}\left[\frac{t}{2\tau}\right] , \tag{12}$$

where τ is given by Eq. (3) and $\tilde{\Phi}(t)$ denotes the complex error function

$$\tilde{\Phi}(t)=\int_0^t dx\ \exp(x^2) . \tag{13}$$

From (12) one readily verifies the short-time expansion

$$\phi_1^f(t)=1-\frac{1}{2}\frac{t^2}{\tau}+O(t^4) \tag{14}$$

and a long-time algebraic decay

$$\phi_1^f(t)=-\frac{2\tau^2}{t^2}+O(1/t^4) . \tag{15}$$

For colliding needles, results for $\phi_1(t)$ as obtained from computer simulation are given in Figs. 3(a)–3(c). The time scale is logarithmic, spanning several decades. For comparison, the expression (12) for a free rotator ($l\le 1/\sqrt{2}$) is also given. As l is increased, the relaxation of $\phi_1(t)$ becomes more and more sluggish. Near $l\approx 2.7$ the relaxation occurs on a rapidly increasing time scale and is almost blocked on the time scale explored by the simulation. The orientational autocorrelation remains close to unity, which means that the needle orientations are virtually frozen in a very narrow solid angle. However, on a logarithmic time scale, and even for the largest l that was used, $\phi_1(t)$ does not seem to level off. In fact, the slope, $d\phi_1/d(\ln t)$, has a small negative value, which stays virtually constant in a large time interval but does not vanish. As we shall see in Sec. IV B, this slow final relaxation is connected to hopping events in the orientational vector.

It should be noted that this behavior is qualitatively very similar to the relaxation scenario of the dynamical structure factor, which is the key quantity characterizing structural glass formers [3,2,9] near the kinetic glass transition. In the ideal version of mode-coupling theory [2], a saturation of this quantity toward a nonvanishing plateau value is predicted and associated with ergodicity breaking in the system. In computer simulations [3,4,21], on the other hand, there is no clear-cut plateau, but thermally activated hopping processes restore ergodicity.

A second dynamical correlation function is that of the angular velocities

$$\psi_1(t)=\left\langle \frac{1}{N}\sum_{i=1}^{N}\vec{\omega}_i(0)\cdot\vec{\omega}_i(t)\right\rangle . \tag{16}$$

For a free rotator, $\psi_1(t)$ is simply

$$\psi_1(t)\equiv\psi_1^f(t)=\langle\vec{\omega}^2(0)\rangle=1/\tau^2=\text{const} . \tag{17}$$

In Fig. 4, $\psi_1(t)$ is shown as a function of l. For increasing l, $\psi_1(t)$ decays more and more rapidly to zero, since the

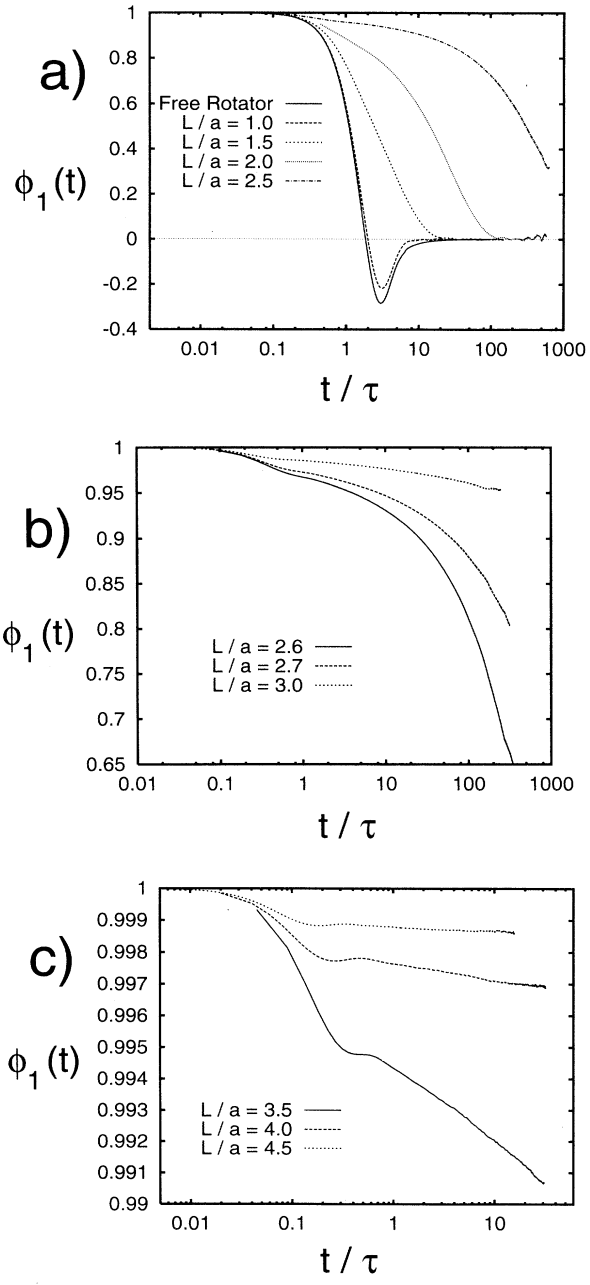

FIG. 3. Orientational autocorrelation function $\phi_1(t)$ versus reduced time t/τ on a logarithmic time scale for different values of $l=L/a$. Note the increasing scale for $\phi_1(t)$. (a) Free rotator ($l\le 1/\sqrt{2}$), $l=1.0$, 1.5, 2.0, 2.5. (b) $l=2.6$, 2.7, 3.0. (c) $l=3.5$, 4.0, 4.5.

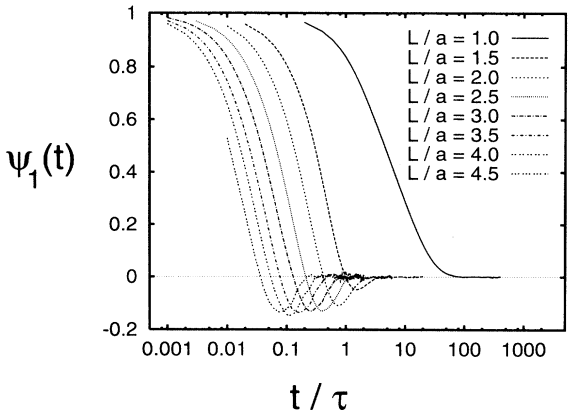

FIG. 4. Same as Fig. 3 but now for the angular velocity autocorrelation function $\psi_1(t)$.

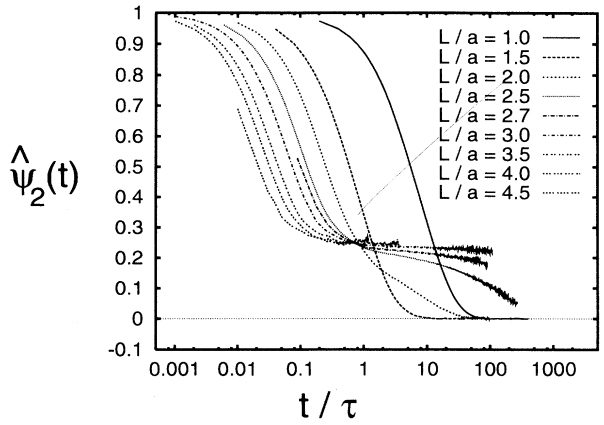

FIG. 5. Same as Fig. 4 but now for the angular velocity autocorrelation function $\hat{\psi}_2(t)$.

number of collisions that destroy correlations in the angular velocity increases. However, the angular velocity correlation is not suited for a clear-cut diagnostic for an orientational glass transition.

A function that is much more sensitive to freezing of needle orientations is obtained by considering the second Legendre polynomial for the direction of the angular velocity, defined by the unit vector $\hat{\omega}_i(t) \equiv \vec{\omega}_i(t)/|\vec{\omega}_i(t)|$. This function is defined as

$$\hat{\psi}_2(t) = \left\langle \frac{1}{N} \sum_{i=1}^{N} P_2(\hat{\omega}_i(0) \cdot \hat{\omega}_i(t)) \right\rangle , \tag{18}$$

where $P_2(x) = \frac{1}{2}(3x^2 - 1)$ is the second Legendre polynomial. For completely decorrelated unit vectors $\hat{\omega}_i(t)$ and $\hat{\omega}_i(0)$ uniformly distributed on the unit sphere, $\hat{\psi}_2(t)$ vanishes since

$$\hat{\psi}_2(t) = \frac{1}{\pi} \int_0^{\pi} d\theta \sin(\theta) \tfrac{1}{2}[3\cos^2(\theta) - 1] = 0 , \tag{19}$$

θ denoting the angle between $\hat{\omega}_i(t)$ and $\hat{\omega}_i(0)$. However, if the unit vector $\hat{\omega}_i(t)$ only varies in a *two-dimensional* subspace (i.e., on the unit circle), then the result for two completely decorrelated unit vectors $\hat{\omega}_i(t)$ and $\hat{\omega}_i(0)$ is

$$\hat{\psi}_2(t) = \frac{1}{2\pi} \int_0^{2\pi} d\theta \tfrac{1}{2}[3\cos^2(\theta) - 1] = \tfrac{1}{4} . \tag{20}$$

If the orientation of the needles is almost frozen, then the angular velocities only vary in a two-dimensional subspace orthogonal to the orientation vector and the long-time limit of $\hat{\psi}_2(t)$ is $\frac{1}{4}$. If the orientation vector is moving, then the result for $\hat{\psi}_2(t)$ should be zero. We have thus defined a quantity that can sensitively discriminate between frozen orientations, corresponding to a glassy state, and a fluidlike motion of orientation.

Results for $\hat{\psi}_2(t)$ are displayed in Fig. 5. The onset of a plateau is apparent for $l \simeq 2.5$. The plateau becomes more and more pronounced and the saturation value is $\frac{1}{4}$, as expected from our previous considerations. There is a drastic qualitative change in the shape of $\hat{\psi}_2(t)$ between $l = 2.0$ and $l = 2.5$, and the system seems to be frozen-in on the time scale explored by the simulation for $l > 2.7$. Hence we can locate a kinetic orientational glass transition at a ratio $l = l_g \simeq 2.7$. This glass transition is accompanied by a change in the relaxation of the orientational correlations. For $l < l_g$ there is three-dimensional motion of the orientational vector within the time scale of the simulation, whereas the orientation is virtually frozen in a cage dynamically formed by the colliding neighbors for $l > l_g$.

As with the structural glass transition in liquids, the orientational transition is not perfectly sharp but rather is smeared. However, the interval in l during which the dynamics change from fluidlike behavior to a virtually frozen-in motion in a cage is very narrow.

B. Needle trajectories

The picture gained for the orientational kinetic glass transition by studying dynamical correlation functions is supported by watching the actual needle trajectories $\{\vec{u}_i\}$ $(i = 1, \ldots, N)$. In Fig. 6, typical trajectories (projected from the unit sphere onto the plane) are shown for three different values of l, two of which are smaller than l_g: (a) $l = 2.0$, (b) $l = 2.5$, and (c) $l = l_g = 2.7$. Whereas the whole unit sphere is explored rapidly for $l = 2.0$, there is already a significant slowing down for $l = 2.5$. Here the sphere is not completely filled by the trajectory on the time scale of the simulation. For $l = l_g = 2.7$ the orientations remain frozen-in on a large time scale and change through sudden jump processes. Such jumps can be interpreted as escape from a cage formed by the neighbors colliding toward another cage. Note that for such a system, the jumps cannot be described as "thermally" activated, since the bottleneck that separates two configurations in phase space is of a purely entropic nature. Here a connection to random walks with different waiting-time distributions on different lattice systems may be seen [22].

C. Orientational diffusion

In the orientationally disordered fluid phase, the rotational long-time self-diffusion coefficient D_r is defined via [23]

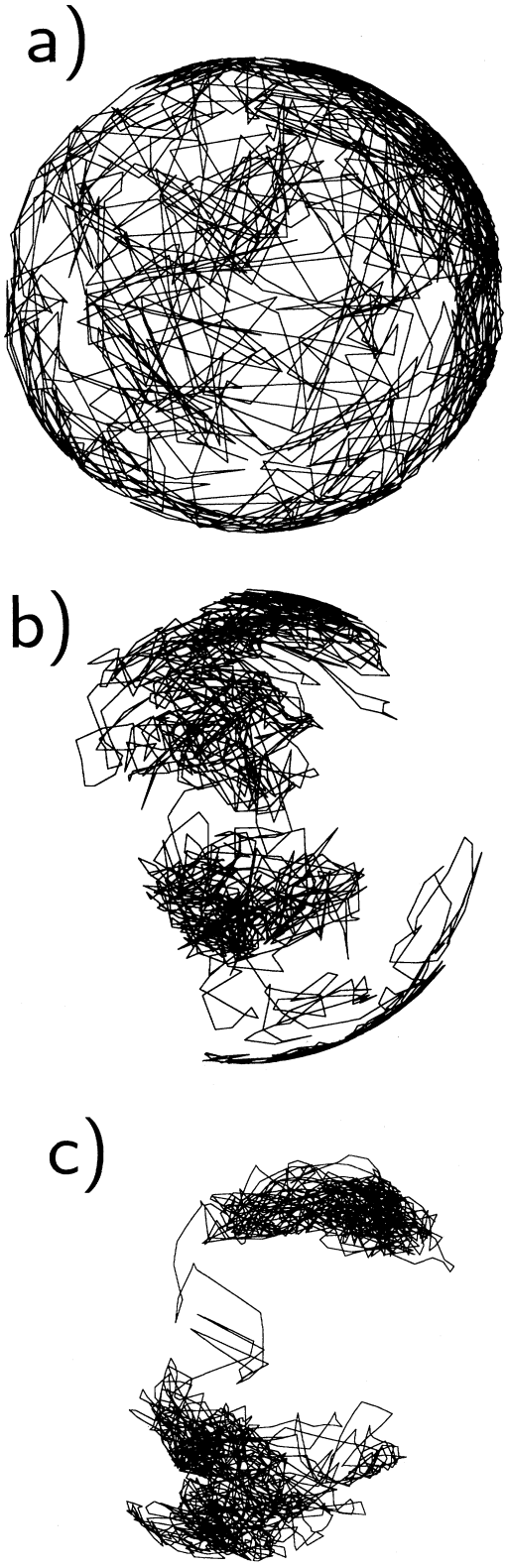

FIG. 6. Typical trajectories of the needle orientations projected from the unit sphere onto the plane. (a) $l=2.0$; here the unit sphere is rapidly explored. (b) $l=2.5$; slightly above the orientational glass transition. (c) $l=2.7$; at the orientational glass transition.

$$D_r = \lim_{t\to\infty} -\frac{1}{2t}\ln[\phi_1(t)] \ . \tag{21}$$

For free rotators, D_r obviously does not exist. In the disordered phase of interacting rods with a translational degree of freedom, D_r is believed to exist [23], although a rigorous mathematical proof is lacking. For $l<l_g$, our numerical results for $\phi_1(t)$ can be described for long times (on the scale of the simulation) by the diffusive behavior proportional to $\exp(-2D_r t)$.

In fragile *structural* glass formers, the temperature dependence of the long-time *translational* self-diffusion coefficient D_t can be described near the kinetic glass transition temperature T_g by a power law

$$D_t(T)=A_t(T-T_g)^{\gamma_t}+\Delta D_t(T) \ , \tag{22}$$

where A_t is an amplitude, γ_t a nonuniversal exponent, and $\Delta D_t(T)$ a small residual distribution resulting from jump diffusion, which restores ergodicity. If one is well above the glass transition, the contribution $\Delta D_t(T)$ is virtually independent of T, and its absolute value can be neglected with respect to the power-law contribution $A_t(T-T_g)^{\gamma_t}$. The expression (22) is supported both by computer simulation [24,21] and mode-coupling theory [25,2]. The exponent γ_t turns out to be 1.4–2.0, depending on the interparticle interaction. It is tempting to check whether a similar law holds for the rotational diffusion constant as a function of l:

$$D_r(l)=A_r(l_g-l)^{\gamma_r}+\Delta D_r \ . \tag{23}$$

If one ignores the small residual diffusion ΔD_r, a log-log plot of D_r versus l_g-l should fall on a straight line. Indeed, taking $l_g=2.7$, the power law describes the results well, except for small l, as shown in Fig. 7. The exponent γ_r turns out to be rather large, $\gamma_r\simeq 4.2$, compared to the values obtained for structural glasses. In any case, the limited range of the data makes it difficult to accurately check a three parameter law such as (23).

For $l>l_g$, the long-time data for $\phi_1(t)$ significantly de-

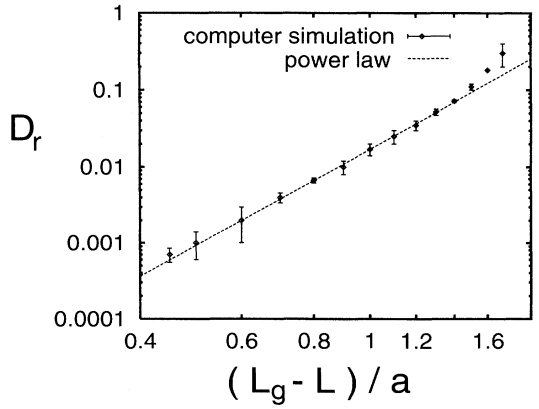

FIG. 7. Rotational diffusion constant D_r versus $l_g-l\equiv(L_g-L)/a$ on a double logarithmic plot. The statistical error from the data is indicated by the error bars. The best power-law fit is shown by the straight dashed line.

viate from a diffusive behavior proportional to $\exp(-2D_r t)$. A better fit is obtained if a stretched exponential proportional to $\exp(t/t_0)^{\nu}$, with $\nu \simeq 0.5$, is used. But again this fit is not the only one that is possible. A simple linear law proportional to $\ln(t)$ can also be used to fit the data quite well in the long-time regime.

V. ORIENTATIONAL GLASS TRANSITION IN A CONFINING GEOMETRY

We have extended the rotator model to a situation where the system is confined by two parallel planar walls separated by a distance h. To model such a confining geometry, a rectangular simulation box with periodic boundary conditions in the x and y directions was used. The boundary conditions in the z direction were either "open" or "free" boundary conditions (simulating a free interface) or "frozen" boundary conditions with fixed, randomly oriented needles beyond the boundary. The two situations are sketched in Fig. 8. For open boundary conditions, the needles at the boundary are much more mobile than those in the bulk, since the number of possible colliding neighbors is drastically reduced. However, for frozen boundary conditions, the mobility of the needles near the boundary is expected to be slightly reduced compared to the bulk mobility. The reason is that—although the number N_N of possible colliding neighbors is the same—the colliding needles are fixed in space and time. The fixed needles can be viewed as needles with an infinite moment of inertia. Then it is straightforward to modify the collision dynamics described in Sec. II B.

The question is whether, and how, the presence of the boundaries influences the orientational glass transition in the "bulk," i.e., in the layers in between the walls that possess the regular bulk number N_N of rotating collision partners. We have performed simulations for $l = L/a = 3$ and $h = 6a$ with a total number of $N = 600$ rotating needles in the simulation box. In Fig. 9, the orientational autocorrelation function $\phi_1(t)$ is shown for different layers in the case of "open" boundary conditions. As expected, in the outermost layers, the correlation decays faster to zero than that belonging to a bulk system. However, in the inner layers, the decay scenario is very similar to and

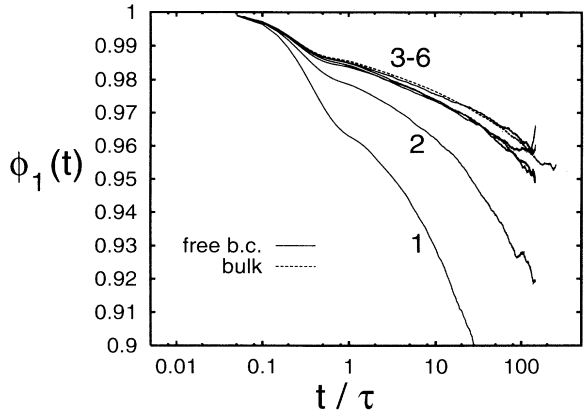

FIG. 9. Layer-resolved orientational autocorrelation function $\phi_1(t)$ versus reduced time t/τ on a logarithmic time scale for open boundary conditions. The parameters are $l = 3$, $h = 2L$. Altogether there are 12 different parallel layers between the walls, two of which are symmetric. Hence we have six different layers, which are a distance $a/2$ apart form each other and are successively labeled by numbers. The outermost layer is labeled 1; the layer in between the plates is labeled 6. For comparison the bulk result is also shown by the dashed line.

virtually indistinguishable from the bulk behavior. The situation is even more striking for "frozen" boundary conditions, where the decay of the orientational correlation in each layer virtually coincides with the bulk result; see Fig. 10. Therefore the only relevant parameter determining the decay of dynamical correlations is the number N_N of possible collision partners. Particularly, as far as a layer far from the boundary is concerned, the orientational glass transition is not changed with respect to the bulk glass transition. It occurs at the same ratio $l = l_g$ as in the bulk system.

This conclusion may be unexpected since recent experiments report on considerable shifts in the glass transition temperature of thin liquid films with respect to the bulk glass transition temperature [14–16]. Also a computer simulation for soft spheres between soft parallel walls [17]

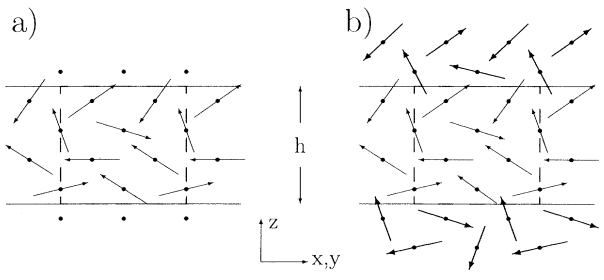

FIG. 8. Schematic view of a two-dimensional cut through the simulation box together with the confining walls for different boundary conditions. The plates have a distance h. (a) "Open" boundary conditions. There are missing neighbors near the boundary. (b) "Frozen" boundary conditions. The thick needles beyond the boundary are completely frozen-in.

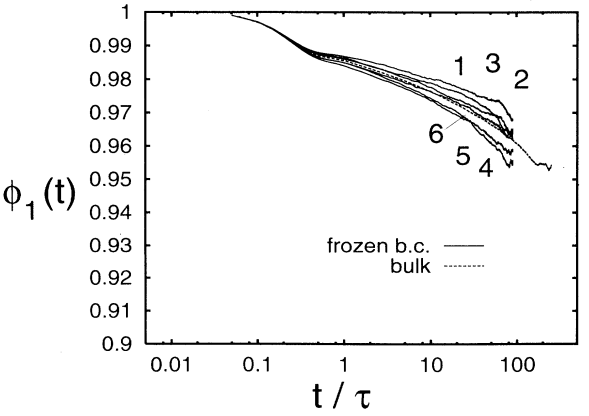

FIG. 10. Same as Fig. 9 but now for frozen boundary conditions.

reveals a significant increase in the glass transition temperature. The physical reason lies in the fact that the system builds well-defined microscopically sharp layers in between the walls, and therefore the mobility of the particles is drastically influenced by the confining geometry. This effect is obviously not contained in our model. Here the discrete layer structure of the center-of-mass coordinates is prescribed and the orientational degree of freedom exhibits a glass transition that is not influenced by the presence of confining geometries. A different effect might be obtained from different types of boundaries (e.g., hard walls favoring a planar orientation of the needles).

VI. DISCUSSIONS AND OUTLOOK

In summary, we have calculated dynamical correlation in a rotator model of hard needles by computer simulation for different ratios $l=L/a$. As l is increased, the system exhibits a "kinetic glass transition," which manifests itself as a crossover from hydrodynamic (diffusive) relaxation of orientation correlations toward a slow relaxation mediated by hopping processes. The actual value for the glass transition was estimated to be $l_g=2.7\pm0.2$. The whole scenario is therefore very similar to the structural kinetic glass transition in simple liquids. The glass transition is mainly dominated by the local number of possible colliding neighbors. Hence, in a confined geometry, the glass transition is not shifted toward different values with respect to the bulk transition, as long as the confining plates are not very close.

The main result of this paper is that, in agreement with the suggestion by Rubinstein and Obukhov [1], a kinetic glass transition may also occur in a very simple system, with a trivial phase diagram. The glass transition, which in that case is detected by a very slow relaxation of the orientational correlations, is hence not necessarily a nonequilibrium phenomenon with a metastable amorphous phase. In the model, there is no intrinsic structural bulk transition but still a dynamical glass transition. This fact casts serious doubts onto earlier approaches to the glass transition that viewed it as related to an underlying bulk phase transition with a diverging correlation length [26,27]. Conversely our study confirms that the glass transition is a purely dynamical effect. The latter conclusion was also anticipated by mode-coupling studies [2], where a continuous static input from the disordered phase leads to a dynamical transition with ergodicity-breaking.

We finish with two general remarks. First, there is certainly a need to construct a mode-coupling theory for the simple needle model in order to check whether the dynamical anomaly can be captured theoretically by using this approach. The construction of such a theory could be similar to mode-coupling approaches applied to conventional orientational glass formers; see, e.g., Michel [28]. Mode-coupling theories, however, are based on the existence of a nontrivial static structure in the system. This nontrivial structure serves as a control parameter for triggering the dynamical instability that is interpreted as a glass transition. It would be interesting to see whether the trivial structural correlations of the rotator model still allow for such instabilities within the mode-coupling approach.

Second, we would like to stress that experiments on confined orientational glasses might be of interest in order to clarify the role of boundaries in glass formation. According to the result of Sec. V, this role might be quite different for orientational glasses and structural glasses. In this respect, one experimental attempt was recently published [29] in which a liquid crystal confined in a porous glass was investigated.

ACKNOWLEDGMENTS

We are indebted to T. Fehr (Physics Department, University of Munich) for helpful discussions and to M. Rubinstein (Eastman Kodak, Rochester) for useful correspondence. This work was supported by the French-German PROCOPE exchange program under Contract No. 312-pro-93-as.

[1] M. Rubinstein and S. P. Obukhov (unpublished).
[2] W. Götze, in *Liquids, Freezing and the Glass Transition,* edited by J. P. Hansen, D. Levesque, and J. Zinn-Justin (North-Holland, Amsterdam, 1991).
[3] J. P. Hansen, Phys. World **4** (12), 32 (1991).
[4] J. L. Barrat and M. L. Klein, Annu. Rev. Phys. Chem. **42**, 23 (1991).
[5] U. T. Höchli, K. Knorr, and A. Loidl, Adv. Phys. **39**, 405 (1990).
[6] K. Binder and J. O. Reger, Adv. Phys. **41**, 547 (1992).
[7] For a recent experimental study, see D. L. Leslie-Pelecky and N. O. Birge, Phys. Rev. B **50**, 13 250 (1994).
[8] *Liquids, Freezing and the Glass Transition,* edited by J. P. Hansen, D. Levesque, and J. Zinn-Justin (North-Holland, Amsterdam, 1991).
[9] H. Löwen, Phys. Rep. **237**, 249 (1994).
[10] W. van Megen and S. M. Underwood, Phys. Rev. E **49**, 4206 (1994).
[11] W. G. Hoover and F. H. Ree, J. Chem. Phys. **49**, 3609 (1968).
[12] P. Ray and K. Binder, Europhys. Lett. **27**, 53 (1994).
[13] J. Baschnagel, K. Binder, and H. P. Wittmann, J. Phys. Condens. Matter **5**, 1597 (1993).
[14] J. Zhang, G. Liu, and J. Jonas, J. Phys. Chem. **96**, 3478 (1992).
[15] J. L. Keddie, R. A. L. Jones, and R. A. Cory, Europhys. Lett. **27**, 59 (1994).
[16] P. Pissis, D. Daoukaki-Diamanti, L. Apekis, and C. Christodoulides, J. Phys. Condens. Matter **6**, L325 (1994).
[17] T. Fehr and H. Löwen, Phys. Rev. E **52**, 4016 (1995).
[18] D. Frenkel and J. F. Maguire, Phys. Rev. Lett. **47**, 1025 (1981); Mol. Phys. **49**, 503 (1983).
[19] C. Renner, diploma thesis, University of Munich, 1995 (unpublished).
[20] M. P. Allen and D. J. Tildesley, *Computer Simulation of Liquids,* Oxford Science Publications (Clarendon, Oxford,

1987).
[21] H. Löwen, J. P. Hansen, and J. N. Roux, Phys. Rev. A **44**, 1169 (1991).
[22] See, e.g., J. Haus and K. W. Kehr, Phys. Rep. **150**, 263 (1987).
[23] M. Doi and S. F. Edwards, *The Theory of Polymer Dynamics,* Oxford Science Publications (Clarendon, Oxford, 1986).
[24] J. N. Roux, J. L. Barrat, and J. P. Hansen, J. Phys. Condens. Matter **1**, 7171 (1989); J. L. Barrat, J. N. Roux, and J. P. Hansen, Chem. Phys. **149**, 197 (1990).
[25] U. Bengtzelius, Phys. Rev. A **34**, 5059 (1986).
[26] D. L. Stein and R. G. Palmer, Phys. Rev. B **38**, 12 035 (1988).
[27] J. P. Sethna, Europhys. Lett. **6**, 529 (1988).
[28] K. H. Michel, Z. Phys. B **61**, 45 (1985); **68**, 259 (1987).
[29] G. Schwalb and F. W. Deeg, Phys. Rev. Lett. **74**, 1383 (1995).